[PROC. OF JSCE No. 354/V-2 (Concrete Eng. and Pavements) February 1985]

EVALUATIONS OF EXTERNAL RESTRAINING EFFECT AND PREDICTION METHOD FOR THERMAL CRACKS IN HIGH STRENGTH LIGHTWEIGHT CONCRETE

By Sadamu ONO, Katsuhiko KIMURA**, Takeji OKADA*** and Takayoshi OTA***

There are a number of unsolved problems regarding the control of thermal cracking in massive concrete structures using high strength lightweight concrete. The purposes of the present investigation are to evaluate the degree of external restraint on the basis of experimental data and to examine the prediction method for the thermal crack properties originally developed for normal weight concrete for its application to high strength lightweight concrete.

1. INTRODUCTION

Recent developments of offshore resources and utilization of sea areas have brought about various innovative designs of concrete platforms and barges. Offshore concrete structure requires an adequate buoyancy capacity for its mobility in addition to the strength and durability levels sufficient to resist severe hydrostatic and oceanographic conditions, in particular ice loads in subarctic and arctic regions. These design requirements have promoted the use of high strength lightweight concrete for these concrete members, which are in some cases massive in their dimensions. Furthermore, a concrete mix used for these structures can be characterized by its high content of cementitious material.

Primary concern in the construction using such concrete mix is to control thermal cracks induced by the hydration of cement and by the internal and external restraining effects on the thermal deformations.

Much developmental work has been carried out by the authors in this field of evaluating thermally induced cracks and the assessment of the optimal construction logistics to minimize such adverse effects for normal weight concrete on the basis of an extensive statistical data.

It is the primary objective of this paper to evaluate the thermal crack formation characteristics of high strength lightweight concrete and to verify the applicability of the systematic approach for their predictions, the analytical method originally developed for normal weight concrete. Emphasis is placed in particular on the evaluation of external restraining effect such as underlying hardened concrete at the construction joint.

* Member of JSCE, M. Eng., Technology Department, Shimizu Construction Co., Ltd. (Mori Bldg. No. 43, Mita, Minato-ku, Tokyo)

** Member of JSCE, M. Eng., Development Department, Shimizu Construction Co., Ltd. (Mori Bldg. No. 43, Mita, Minato-ku Tokyo)

*** Member of JSCE, M. Eng., Institute of Technology, Shimizu Construction Co., Ltd. (Etchujima, Koto-ku, Tokyo)

Results of analytical procedures as presented in section 3 of this paper are evaluated by generating analytical parameters, which express the degree of external restraining effect, using results obtained from previously conducted large scale field experiment[1),2)]. These parameters are used in section 4 to predict the thermal crack properties as crack width and crack spacing. The results of these analyses are compared with those actually induced cracks in the experiment.

2. SUMMARY OF THE EXPERIMENTAL DATA[1),2)]

(1) Test specimen

The dimensions and re-bar arrangement of the test specimen used in the large scale field experiment are shown in Fig. 1. Specimen length to height ratio, L/H, is a parameter indicative of the degree of external restraint and the value is approximately 20. The specimen was constructed on the existing concrete slab of approximately 25 m wide, 40 m long and 0.8 m thick supported by pile foundation. The top and end surfaces were insulated with foaming polystyrol and airpack sheets. The test specimen was divided into five blocks and various curing conditions were applied to the side faces of the specimen in order to observe their effects on the thermal characteristics of concrete, as shown in Fig. 2. Curing method for side R of block E as shown in Fig. 2. is by steel forms with polyurethane foam. Side L of block E is with plywood forms. Forms were removed 4 days after concrete placement. Membrane curing compound was then sprayed. Concrete was cured with 3 sheets of airpack for additional 6 to 7 days.

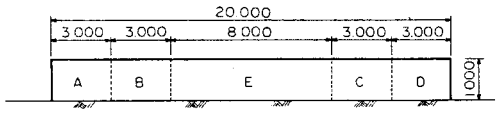

A; steel form only
B; steel form insulated with polyurethane foam (forms not removed)
C; steel form + air inflated vinyl sheet (airpack)
D; steel form + polyethylene sheet
(steel form insulated with polyurethane foam
plywood form is used on the opposite side)

Fig. 2 Curing Methods.

(2) Concrete mix

Mix proportion of the concrete is shown in Table 1. Type of cement used is an ordinary portland cement. Silica fume was blended as its mineral admixture. Chemical admixtures were added to obtain the specified air content and slump.

Table 1 Concrete Mix Proportion.

Max. Agg. Size (mm)	Slump (cm)	Air Content (%)	W/C (%)	S/A (%)	UNIT CONTENT (kg/m³) W	C	S	G	SF	(%, wt. of C+SF) AE-Agent	Super Plasticizers
15	20±3	6±1	32	40	147	460	638	480	46	0.065	2.600

SF : silica fume

(3) Instrumentations

a) Temperature of concrete

Temperature was measured by copper-constantan (C-C) thermocouples embedded at the positions illustrated in Fig. 3, which shows the section at the middle span of the specimen.

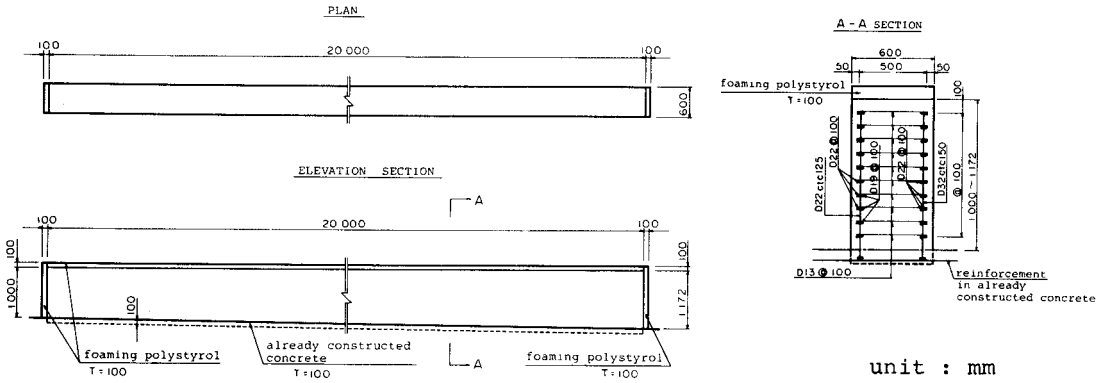

Fig. 1 Dimensions of Test Specimen and Re-bar Arrangements.

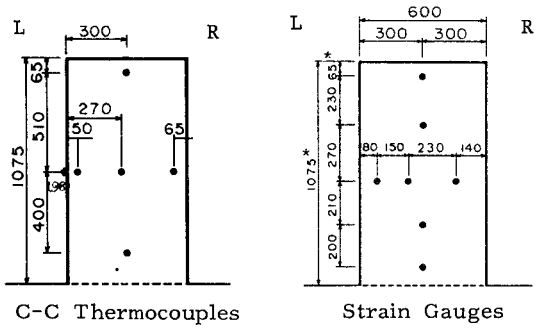

Fig. 3 Location of Measuring Points.

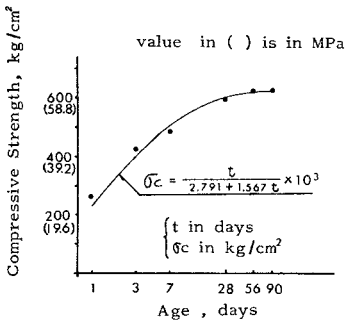

Fig. 4 Compressive Strength.

Table 2 Properties of Fresh Concrete.

	slump	air content	unit weight	temp.
Base concrete	11.1 cm	5.4 %	1.764 t/m³	32.5 ℃
Flowing concrete	21.0 cm	5.9 %	1.772 t/m³	30.5 ℃

Table 3 Properties of Hardened Concrete.

Item \ Age	1	3	7	28	56	90
Compressive strength σc	262 (25.7)	424 (41.6)	486 (47.6)	598 (58.6)	623 (61.1)	628 (61.5)
Tensile strength σct	25.3 (2.48)	33.8 (3.31)	40.3 (3.95)	44.4 (4.35)	44.8 (4.39)	49.5 (4.85)
Young's modulus Ec	--	19.2 (1.88)	20.5 (2.01)	23.0 (2.25)	24.1 (2.26)	23.8 (2.28)

where σc and σct are in kg/cm²
Ec is in 1.0×10⁴kg/cm²
value in ( ) is in MPa
age is in days

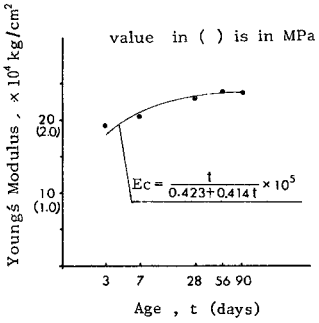

Fig. 5 Young's Modulus.

b) Concrete strain

Strain was measured by strain gauges. Their positions are also illustrated in Fig. 3.

(4) Properties of concrete

Measured results on the properties of fresh concrete are summarized in Table 2. Properties of hardened concrete ; compressive strength, tensile strength and Young's modulus, are shown in Table 3, Fig. 4 and Fig. 5.

(5) Test results

a) Temperature of concrete

Time-dependent temperature variation is shown in Fig. 6. Maximum internal temperature rise, T_{max}, ranged from 77.8°C to 78.6°C on the three different sections in block E. Temperature reached these values in half a day after placement. Maximum surface temperature rise, $T_{s,max}$, ranged from 70.2°C to 79.0°C in block E on the side R cured using steel forms with polyurethane foam, and approximately 66.5°C on the side L cured using plywood forms. The temperature rise on the side R cured using steel forms with polyurethane foam was 3.4°C to 12.6°C higher than that on the side L cured using plywood forms due to its insulating effect. Maximum difference between internal and surface temperature ranged from 12.9°C to 13.6°C on the three different sections in block E. The difference between internal and surface temperature due to changes in curing materials is about 7°C.

b) Concrete strain

Time-dependent variation in concrete strain is shown in Fig. 7. The values measured at about three hours after the placement of concrete were set to be the initial values. Fig. 7 leads to the following conclusions.

Incremental change in the value of restrained strain, ε_R, in compression at each measuring point increased while temperature continued to rise. However it increased toward tension while temperature

continued to drop.

c) Appearance of cracks

Fig. 8 shows the result of survey on the crack formation at two months after the removal of forms. The maximum value of the measured crack width was 0.16 mm. The average crack width was 0.04 mm. The average crack spacing was 82.7 cm.

3. DEGREE OF EXTERNAL RESTRAINT

(1) Definition of the degree of external restraint

Degree of the restraining effect can be evaluated in terms of either stress or deformation. Further consideration of the actual phenomena can be made by incorporating the effect of creep.

In this paper, the degree of restraint is defined by the equations of the followings, eq. (1) and eq. (6).

a) In case where the degree of restraint is evaluated in terms of stresses,

$$R_s(t)=\frac{\sigma_R(t)}{\sigma'_R(t)} \quad \cdots\cdots (1)$$

where, $R_s(t)$: degree of restraint evaluated in terms of stress at t days

$\sigma_R(t)$: restrained stress of concrete at t days

$$\sigma_R(t)=\int_0^t B(t-t')\cdot E(t')\cdot\frac{d\varepsilon}{dt'}\cdot dt' \quad \cdots\cdots (2)$$

$\sigma'_R(t)$: fully restrained stress of concrete at t days

$$\sigma'_R(t)=\int_0^t B(t-t')\cdot E(t')\cdot\alpha\cdot\frac{dT}{dt'}\cdot dt' \quad \cdots\cdots (3)$$

α : thermal expansion coefficient of concrete

ε : restrained strain of concrete

$B(t-t')$: stress relieving factor due to creep at t days for the load applied at t' days

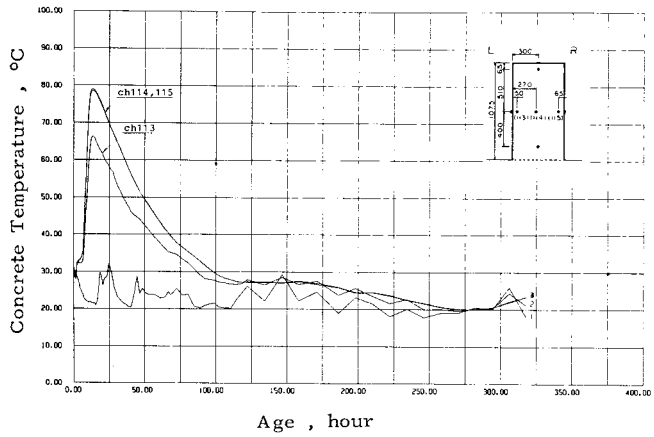

Fig. 6 Time-dependent Temperature Variation.

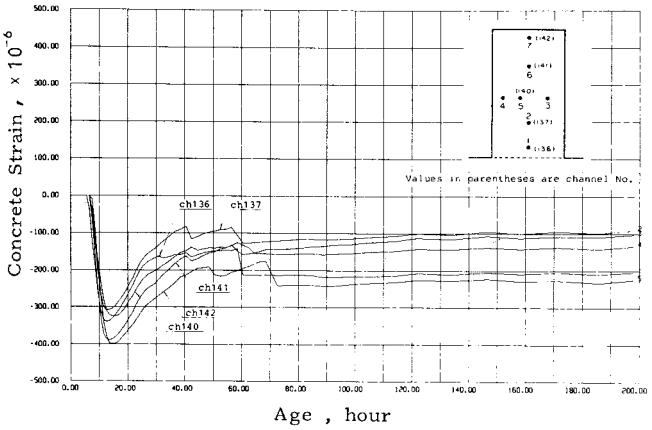

Fig. 7 Time-dependent Concrete Strain Variation.

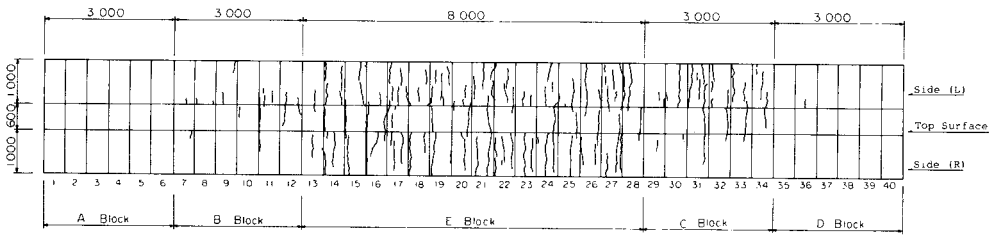

Fig. 8 Unfolded Plan of Cracking.

T : temperature of concrete

The equation (1) can be re-written using a relationship $B(t-t')=\frac{1}{\psi(t-t')+1}$ considering the creep effect, which is identified by subscript 1,

$$R_{s1}(t)=\frac{\int_0^t \frac{E(t')}{\psi(t-t')+1}\cdot\frac{d\varepsilon_R}{dt'}\cdot dt'}{\int_0^t \frac{E(t')}{\psi(t-t')+1}\cdot\alpha\cdot\frac{dT}{dt'}\cdot dt'} \quad \cdots\cdots (4)$$

also, the equation (1) can be re-written using $B(t-t')=1.0$ neglecting the creep effect, which is identified by subscript 2,

$$R_{s2}(t)=\frac{\int_0^t E(t')\cdot\frac{d\varepsilon_R}{dt'}\cdot dt'}{\int_0^t E(t')\cdot\alpha\cdot\frac{dT}{dt'}\cdot dt'} \quad \cdots\cdots (5)$$

b) In case where the degree of restraint is evaluated in terms of strains,

$$R_n(t)=\frac{\varepsilon_R(t)}{\varepsilon'_R(t)} \quad \cdots\cdots (6)$$

where, $R_n(t)$: degree of restraint evaluated in terms of strain at t days

$\varepsilon_R(t)$: restrained strain of concrete at t days

$\varepsilon'_R(t)$: fully restrained strain of concrete at t days

$$\varepsilon'_R(t)=\int_0^t \alpha\cdot\frac{dT}{dt'}\cdot dt' \quad \cdots\cdots (7)$$

(2) Analytical conditions

a) The degree of external restraint, R, is calculated separately for the two different phases ; one in which temperature rises and the other where temperature drops.

b) Equation for the creep coefficient in the eq. (4) is as follows : [3]

$$\psi(t)=\frac{t}{22.96+1.42\,t} \quad \cdots\cdots (8)$$

where, $\psi(t)$: creep coefficient at t days

t : age in days

c) Temperature was measured using strain gauges and the results were used for corrections of measured strains.

d) Calculations for the external restraining effect, R, are carried out for each value of strain measured at each measuring point and for a value of strain averaged in the vertical direction.

e) It is assumed that the distributions of temperature and strain in a vertical direction are represented by a parabola.

f) Thermal expansion coefficient of concrete is to be $10\times10^{-6}/°C$.

(3) Evaluation of the degree of external restraint

Value of R, the external restraining effect, is calculated for each case, and results are shown Fig. 9 and Fig. 10 . Figure 11 shows the time-dependent variation of R in the vertical direction at the middle section.

a) Values of R_s and R_n, calculated in terms of stress and strain respectively, during a phase where temperature continues to rise, are in good agreement. Their values vary between 0.7 and 0.9, indicating high restraining effect and negligibly small variation in the vertical direction. Reasons for this effect are as follows ;

i) When Young's modulus of specimen is smaller than that of the base concrete, elastic restraint is significant.

ii) Stress relaxation due to the effect of creep is small since temperature rise occures in a short time, resulting in a small temperature variation in the vertical direction.

b) Values of R greater than unity have been observed after 0.5 to 1.0 day. This is mainly due to the

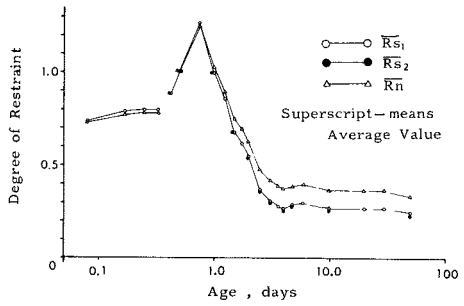

Fig. 9 Time-dependent R Variation (average value).

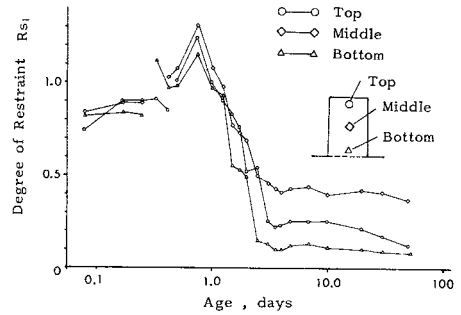

Fig. 10 Time-dependent R Variation (at each point).

possible effect of the internal thermal restraint induced by temperature difference between the outer surface and the inner point. Furthermore, some discrepancies in the recorded value exist, especially at an early stage of the measurement.

c) Values of R_s and R_n from 1 to 1.5 days during a phase in which temperature decreases are nearly in agreement. Difference between R_s and R_n values is about 0.1.

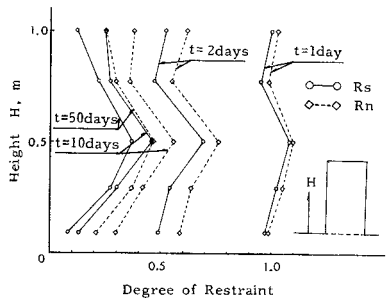

Fig. 11 Time-dependent R Distribution Variation.

d) Drastic reduction in the value of R has been observed at 2 days relative to the value observed at 1 day. This is due to the following factors :

i) Cracks may have occurred near the strain gauges.

ii) Possible slippage on the interface of the specimen and the base concrete. Restrained strain was relaxed due to above causes.

e) Reason why R at the middle height is greater than that at the top and bottom is due to internally restrained strain which is occurred due to temperature difference in the vertical direction.

f) Discrepancy observed in the values of the degree of external restraint, when evaluated in terms of stresses is due to the effect of time-varying increase in the value of the Young's modulus of concrete. Greater values have been recorded when the effect of the external restraint is evaluated in terms of strain and this ratio increases as concrete ages.

4. EVALUATION OF THERMAL CRACK PROPERTIES

(1) Analytical method for the prediction of thermal crack properties[4]

Prediction model for the thermal crack properties such as crack width, crack spacing, and total area of cracks appeared on a concrete surface is described as follows : cracks in the area of L m long and H m high are modeled as shown in Fig. 12.

The analysis for the maximum crack width is based on the result of multi-variate analysis on the visually observed crack data. In this, the maximum crack width, W_{max}, that appears over the surface area of the concreting block, is a function of the length of concreting

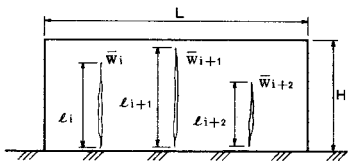

L ; length of block (m)
H ; height of block (m)
$\overline{Wi}$; average crack width
li ; length of each crack (m)
Ai ; area of each crack (mm^2)
$\sum_{i=1}^{N} Ai$; area of whole cracks occurred in area of L by H (mm^2)
MAX ($\overline{Wi}$) ; maximum of average crack widths occurred in area of L by H (mm)
R ; degree of external restraint
N ; number of cracks occurred in area of L by H

Fig. 12 Typical Illustration of Thermal Crack Occurrence.

block, L, degree of the external restraining effect, R, and a statistical parameter, MAC.

$$W_{max}=K\cdot L\cdot R\cdot(MAC) \quad (9)$$

where, K : constant $K=1.59$

R : degree of external restraining effect

L : length of a concreting block (m)

MAC is a function of independent variables, X_i, such as reinforcing steel ratio, as summarized in Table 4 and the corresponding regression coefficients, C_i, such that,

$$MAC=\sum C_i\cdot X_i \quad (10)$$

$$\frac{W_{max}}{W_{ave}}=K \quad (11)$$

where, W_{ave} : maximum average crack width (mm)

The analysis of thermal crack spacing is also based on the result of multi-variate analysis. Average crack spacing, L_c, over the length of concreting block is defined by the parameters MAC and R and a statistical parameter UCA as,

$$L_c=\frac{1000\cdot L\cdot R\cdot(MAC)}{(UCA)+1000\cdot R\cdot(MAC)} \quad (12)$$

$$TA=L\cdot H\cdot(UCA) \quad (13)$$

where, TA : total crack area (mm^2)

UCA is a function of independent variables, Y_i, and regression coefficients, D_i, as summarized Table 5, such that,

$$UCA=\sum D_i\cdot Y_i \quad (14)$$

(2) Comparison of analytical and experimental results

Analytical data for MAC is shown in Table 6. From this result, W_{max} is calculated as follows for the values of $K=1.59$, $L=20$ m, $R=0.22$ (0.32), and $MAC=0.016$.

$W_{max}\fallingdotseq 0.11$ mm (based on stress)

$W_{max}\fallingdotseq 0.14$ mm (based on strain)

R is an averaged degree of external restraint at an age of 50 days. The value is obtained from Fig. 11. The average width, W_{ave}, is calculated from eq. (11).

$W_{ave}=0.11/1.59\fallingdotseq 0.07$ mm

(based on stress)

Table 4 Independent variables and Regression Constants for MAC.

$MAC=\sum Ci\cdot Xi$

INDEPENDENT VARIABLES, Xi		REGRESSION CONSTANTS, Ci ($\times 10^{-3}$)
X_0	CONSTANT (1.0)	−0.56
X_1	CONCRETING BLOCK LENGTH (m)	−0.02
X_2	CONCRETING LIFT (m)	−0.55
X_3	DEG. OF EXT. RESTRAINT, R	−17.70
X_4	REINFORCEMENT RATIO (%)	−24.40
X_5	SLUMP (cm)	1.54
X_6	UNIT CEMENT CONT. (KG/CU.M)	0.07
	CONCRETING SEASONAL FACTORS	
X_7	SUMMER (1.0), IF NOT (0.0)	8.13
X_8	AUTUMN (1.0) —DIT—	−3.71
X_9	WINTER (1.0) —DIT—	−6.21
X_{10}	DROP IN TEMPERATURE (°C)	0.33
X_{11}	WALL THICKNESS (m)	−3.18

(Sample Size N = 130)

Table 5 Independent variables and Regression Constants for UCA.

$UCA=\sum Di\cdot Yi$

INDEPENDENT VARIABLES, Yi		REGRESSION CONSTANTS, Di
Y_0	CONSTANT (1.0)	−44.40
Y_1	CONCRETING LIFT (m)	− 0.52
Y_2	REINFORCEMENT RATIO (%)	−19.08
Y_3	CONTROL JOINT (EXIST 1.0, IF NOT 0.0)	−54.72
Y_4	SLUMP (cm)	3.52
Y_5	PLACING TEMPERATURE (°C)	0.17
	CONCRETING SEASONAL FACTORS	
Y_6	SUMMER (1.0), IF NOT (0.0)	0.81
Y_7	AUTUMN (1.0). —DIT—	−26.30
Y_8	WINTER (1.0), —DIT—	−18.37
Y_9	MAX. SURFACE TEMP. RISE (°C)	0.82
Y_{10}	INTERNAL AND SURFACE TEMP. DIF. (°C)	1.88
Y_{11}	DROP IN TEMPERATURE (°C)	0.78

(Sample Size N = 130)

Table 6 Results of *MAC* Calculation.

Section No. \ Factor	*1 L (m) X1	*2 H (m) X2	R (Short Period) X3	*3 P (%) X4	Slump (cm) X5	*4 C (kg/m^3) X6	Placing Time of Concrete: Summer X7	Autumn X8	Winter X9	ΔTm^t (Short Period) (°C) X10	Wall Thickness W (m) X11	MAC (mm/m)
4	20.0	1.0	0.22	2.41	21.0	506	0	1	0	54.6	0.6	0.016
			0.32									0.014

Column *1 Larger Dimension of Concrete Block
*2 Smaller Dimension of Concrete Block
*3 Transverse Reinforcement Ratio
*4 Unit Cement Content

Table 7 Results of *UCA* Calculation.

Section No. \ Factor	Short Side Length H (m) X1	*1 P (%) X2	Control Joint X3	Slump (cm) X4	*2 Tp (°C) X5	Placing Time of Concrete: Summer X6	Autumn X7	Winter X8	Ts, r, max X9 (°C)	Δ Ts, max X10 (°C)	ΔTm^t (short period) X11 (°C)	UCA (mm^2/m^2)
4	1.0	2.41	0	21.0	30.6	0	1	0	37.0	8.4	54.6	50.64

Column *1 Transverse Reinforcement Ratio
*2 Temperature of Concrete

$W_{ave}=0.14/1.59\fallingdotseq 0.09$ mm
(based on strain)

The histograms of the crack widths and average crack widths measured in the test specimen are shown in Fig. 13 and Fig. 14. As seen in Fig. 13 and Fig. 14, W_{max} is 0.16 mm and W_{ave} is 0.08 mm. The experimental results agree well with the calculated results using values of R evaluated by the two different methods in terms of stress and strain. The calculated results using R_n (degree of restraint evaluated in terms of strain) give fairly good agreement with the experimental results. Within the limit of this experiment, it is recognized that R_n evaluated in terms of strain can satisfactorily represent W_{max} and W_{ave}. Furthermore, differences in W_{max} and W_{ave} between the

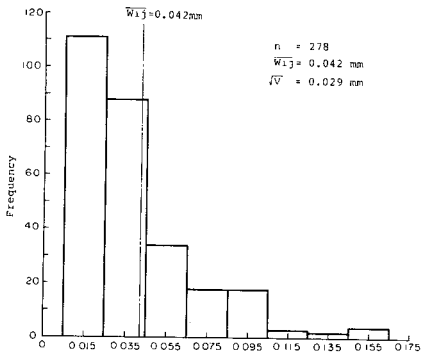

Fig. 13 Frequency of Crack Width at each Measuring Point.

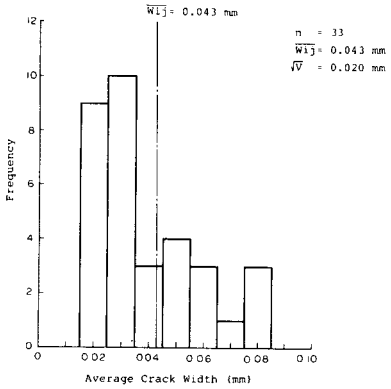

Fig. 14 Frequency of Average Crack Width.

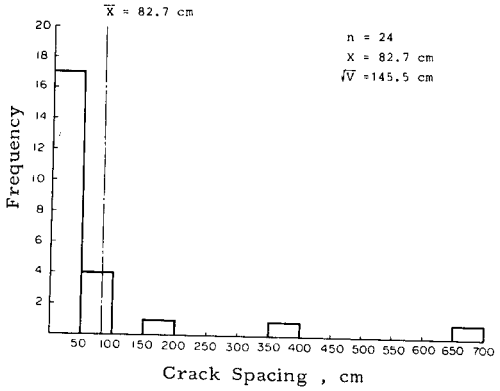

Fig. 15 Frequency of Crack Spacing.

experimental and the calculated results are from 2/100 to 5/100 mm and 1/100 mm respectively. Considering the order of crack width deviation in the prediction is 1/100 mm, Ono's method[4] developed for normal weight concrete is thought to be applicable for high strength lightweight concrete.

$L_c = (1\,000 \times 0.22 \times 20 \times 0.016) / (50.64 + 1\,000 \times 0.22 \times 0.016)$

$\fallingdotseq 1.30$ m (based on R_s)

$L_c = (1\,000 \times 0.32 \times 20 \times 0.014) / (50.64 + 1\,000 \times 0.32 \times 0.014)$

$\fallingdotseq 1.63$ m (based on R_n)

The histogram of crack spacings measured in the test specimen is shown in Fig. 15. As seen in the figure, L_c is about 0.83 m. Some discrepancy among the analytical and experimental results is recognized. L_c calculated using R_n is larger than L_c calculated using R_s.

4. CONCLUSION

The followings have been clarified after the investigation of the degree of external restraint and the evaluation of thermal crack properties in high strength lightweight concrete.

(1) Degree of external restraint for high strength lightweight concrete using rich mix proportion is significant in the early age, and it decreases as time elapses. Furthermore, degree of external restraint is almost constant after a certain age.

(2) R_n in terms of strain and R_s in terms of stress are nearly equal, however it is recognized that R_n tends to show higher values than R_s.

(3) Prediction model of thermal crack properties for normal weight concrete proposed by Ono[4] can be applied to high strength lightweight concrete. This was experimentally verified.

(4) Degree of external restraint in the case of predicting the maximum crack width and average crack width should be assessed using R_n which is evaluated in terms of strain.

5. ACKNOWLEDGEMENT

The authors wish to thank Dr. Shigeyoshi Nagataki (Prof. Tokyo Institute of Technology) for his helpful advices.

REFERENCES

1) Ono, Y., Suzuki, T., Niwa, M. and Iguro, M. : On the Development of Light Weight Concrete for Arctic Application Concrete Island Drilling System, Cement & Concrete, No. 450, Aug. 1984.

2) James F. McNary, Nakajima, T., Iguro, M., Ono, S. and Inoue, K. : Control of Thermal Cracking in the Construction of Offshore Concrete Structure, ACI Fall Convention, 1984.

3) Nishibayashi, S., Kobayashi, K. and Ono, K. : Studies on Concrete using Artificial Light Weight Aggregate, Review of the 19 th General Meeting of Cement Association of Japan.

4) Ono, S., Nakura, K. and Kanamori, H. : Numerization of thermal cracks in massive concrete structure, Preprint of the 38 th Annual Meeting of JSCE, No. 5, Sep. 1983.

(Recieved August 2 1984)